GEOLOGY | THE GEOLOGICAL SOCIETY OF AMERICA®

https://doi.org/10.1130/G51730.1

Manuscript received 13 September 2023
Manuscript accepted 2 October 2023

Published online 12 October 2023

Origin of paired extension-compression during rotational rifting: An early Paleogene example from the northeast Atlantic region and its implications

Po Wan Wong*, Ivar Midtkandal, and Jan Inge Faleide
Department of Geosciences, University of Oslo, P.O. Box 1047, Blindern, N-0316 Oslo, Norway

ABSTRACT

The formation of paired extension-compression (PEC) postulated by rotational kinematics of rift propagation is demonstrated by analogue models but rarely observed in nature. In our study of the early Paleogene continental rift in the northeast Atlantic, a PEC is proposed based on the northeastward propagation and the coeval compression at the rift tip. The propagation is deduced from tectono-magmatic trends, including along-axis development of magmatism, and migration of tectonic faulting inward and toward the rift tip. Where this propagation terminated, we documented coeval extension and compression in the form of a horst-and-graben system (H&G) and V-shaped anticline (VA), respectively. Given their structural characteristics and spatiotemporal relationships with the rift, their origin is best illustrated by a three-stage model: (1) Rifting initiated at the site of mantle upwelling and propagated northeastward in the Paleocene. (2) The rift tip was stalled by an elevated mafic-ultramafic body at the Barents Shelf, which led to forward projection of the rift's driving force to create the H&G and the VA (PEC), dissipating the along-axis force component. (3) Domination of axis-perpendicular components then promoted orthogonal extension and sheared margin development. Our study suggests that PEC has a crucial role in both termination of propagation and rift-mode conversion.

INTRODUCTION

Rift propagation is defined as growth of the axial length through continual stretching and rupturing of lithosphere in front of the rift tip (Fig. 1A). Once rifting starts due to hotspot activity or plate divergence, asthenospheric mantle rises in the form of flows (Huismans and Beaumont, 2011). Continuous flows in the rift maintain a dynamic mass of upwelling mantle (Fig. 1A), which exerts gravitational stress in both the along-axis and axis-perpendicular directions to drive propagation (Mondy et al., 2018). Since mantle flows decrease toward the rift's tip due to the combined effects of viscous friction and narrowing of the rift conduit (Phipps Morgan and Parmentier, 1985), gravitational stress diminishes along the rift axis, causing a differential extension rate in the rotational kinematics (Fig. 1A). Given that a propagating rift has nonzero angular velocity ($\omega > 0$), the pivot of rotation (PR; $r = 0$) is by default at the rift tip, where no deformation takes place ($V = 0$) (Fig. 1A).

In theory, these rotational kinematics would project the rift's driving force forward (Hey et al., 1980; Martin, 1984), leading to paired extension-compression (PEC) (Fig. 1B). In analogue models, PEC is demonstrated as concurrent rifting and thrusting in the two opposite sectors of the PR (Fig. 2A) (Zwaan et al., 2020; Schmid et al., 2022). In nature, however, PEC is uncommon. Propagating rifts in Iceland and the Galapagos Rise, for example, are not marked with observable folding or uplift. Even in the cases of Woodlark Basin and the Taupo Rift, where synrift compression is observed in front of the rift, both the compression and the rotational extension are instead the results of subduction-accretion (Ott and Mann, 2015; Wallace et al., 2009). Global positioning system (GPS) data from the Arctic–NE Siberia region (Hindle et al., 2009), however, tend to indicate ongoing PEC, where the Gakkel Ridge–Laptev Rift is under rotational extension, and the Okhotsk plate is under coeval compression. The circumstances under which a propagating rift would create PEC are, therefore, a conundrum.

The aim of this study was to establish a natural example of PEC, as illustrated by a horst-and-graben system and a V-shaped anticline in the SW Barents Shelf. We first clarified the context of early Paleogene rift propagation in the NE Atlantic. Using seismic and wellbore data, we then defined the ages and structural characteristics of the PEC structures. Their relationships with the rift were delineated through an integrated analysis before we investigated the PEC's origin and implications.

Early Paleogene Rift Propagation in the Northeast Atlantic

The PEC of this study is located at the SW Barents margin bounding the early Paleogene Northeast Atlantic Rift (NAR) (Fig. 2B). As indicated by the younging trend of volcanics (Larsen et al., 2014), the continental rift likely propagated northeastward. The viability of this scenario was examined through a detailed reconstruction of the NAR's configuration, based on recently published structural data and the ages of igneous units compiled by Wilkinson et al. (2017) (refer to Supplemental Material[1]). Based on the tectono-magmatic trends, a three-stage evolution of the NAR was identified (Fig. 2C) and compared with analogue model results.

Stage 1—Rift Initiation (ca. 66–59 Ma)

Stage 1 was characterized by a bimodal pattern (Fig. 2B). Magmatism (area in purple, Fig. 2B), which started at ca. 63 Ma, was

Po Wan Wong https://orcid.org/0000-0002-4352-5304
*p.w.wong@geo.uio.no

[1]Supplemental Material. Data source of the tectono-magmatic trends of the early Paleogene continental rift at the NE Atlantic region (prior to breakup at ca. 54 Ma). Please visit https://doi.org/10.1130/GEOL.S.24263023 to access the supplemental material, and contact editing@geosociety.org with any questions.

CITATION: Wong, P.W., et al., 2024, Origin of paired extension-compression during rotational rifting: An early Paleogene example from the northeast Atlantic region and its implications: Geology, v. 52, p. 27–32, https://doi.org/10.1130/G51730.1

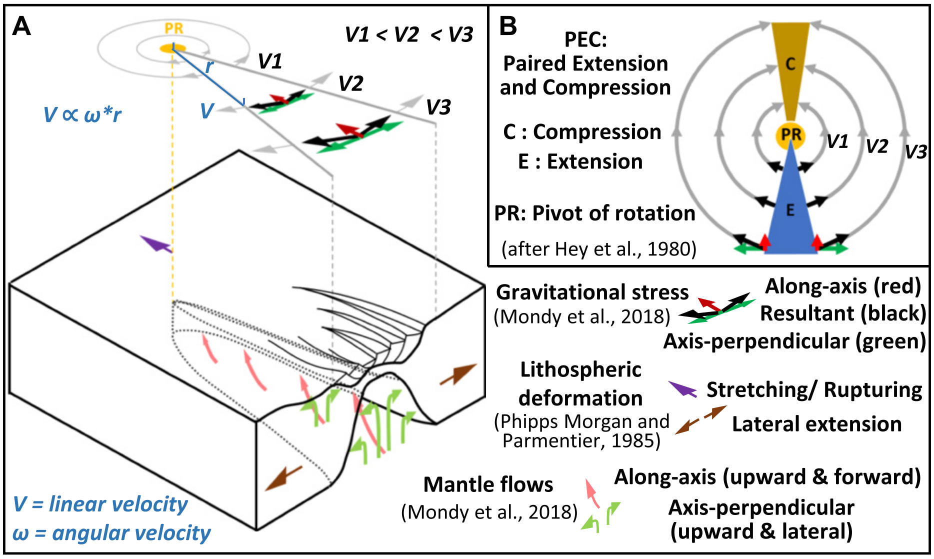

Figure 1. (A) Conceptual model showing various aspects of rift propagation. (B) Paired extension-compression (PEC) and rotational kinematics.

confined to the SW by the Shetland–Faroe Island–Kangerlussuaq lineament (Storey et al., 2007; Hansen et al., 2009; Larsen et al., 2014; Jolley et al., 2021). Early Paleocene normal faults are found to the NE, at the Vøring-Lofoten margin (Zastrozhnov et al., 2020; Meza-Cala et al., 2023) and the Thetis Basin (Fyhn et al., 2021). The area in between was inactive, as shown by the lack of early Paleocene faulting at the Møre shelf (Lundin and Dore, 2019). The configuration of this stage resembles the initiation phase of the analogue model by Schmid et al. (2022), in which rapid growth of a first-generation rift is seen in two separated sets of segments (Fig. 2A). This stage ended with a volcanic hiatus at ca. 59–58 Ma (Jolley et al., 2021).

Stage 2—Rift Propagation (ca. 58–54 Ma)

In stage 2, the magmatic rifting domain and the tectonic faulting domain grew rapidly and extensively along the axis (phase 1) and eventually merged (phase 2) (Figs. 2B and 2C). In phase 1 (ca. 58–55 Ma), tectonic faulting took place in major basins to the NE (Zastrozhnov et al., 2020; Fyhn et al., 2021; Meza-Cala et al., 2023) and to the SW (Stoker et al., 2017). Magmatic rifting was most intense in the middle (Fig. 2B), producing plateau lava in the Blosseville–Jan Mayen area (Storey et al., 2007; Larsen et al., 2014; Blischke et al., 2022) and extensive intrusions and lava fields in the Vøring-Møre area (Svensen et al., 2010; Gernigon et al., 2020). Reactivation of the Faroe–NE Rockall area was marked by widespread igneous activity (Jolley et al., 2021; Walker et al., 2022). The bidirectional growth of magmatic rifting (area in blue, Fig. 2B) is comparable to the development of a second-generation rift in the analogue model (Fig. 2A).

In phase 2 (ca. 55–54 Ma), the locus of magmatism migrated both northeastward and inward and merged with the faulting domain (Fig. 2B). Associated with the volcanic outer high (Geissler et al., 2017), lavas and intrusions filled the rifts at the Lofoten shelf and Thetis Basin (Fyhn et al., 2021; Meza-Cala et al., 2023). Localization of rifting created a narrow zone of thinned crust and melt production (Gernigon et al., 2020), giving rise to the region's earliest seaward-dipping reflector (SDR) units along the future line of breakup (Abdelmalak et al., 2016; Franke et al., 2019; Blischke et al., 2022). The overall pattern (area in green, Fig. 2B) is similar to the late-stage configuration of the propagation model, in which various segments of all rift generations are activated simultaneously (Fig. 2A).

Stage 3—Breakup and Seafloor Spreading (from ca. 54 Ma)

Stage 3 started when breakup and associated sheared margin formation occurred in the early Eocene (Faleide et al., 2010). On a regional scale, opening of the Norwegian-Greenland Sea (NGS) was largely orthogonal, as the C24n.3n chron (53.93 Ma) segments show strong parallelism on both ends (Gaina et al., 2017). Discontinuities and curvatures of these chrons in the Thetis Basin–Lofoten areas and the Aegir Ridge are interpreted to record local-scale southwestward propagation that started at the Senja Fracture Zone (SFZ) and the Jan Mayen Fracture Zone (JMFZ), respectively (Fig. 2C) (Franke et al., 2019; Gernigon et al., 2020).

Driving Force of NAR Propagation

As the NE Atlantic was not affected by any subduction in the early Paleogene, the driving force of the NAR's propagation can be attributed to differential gravitational stress inside the rift conduit. To the southwest of the Bivrost Lineament (BL), the excessive magmatic (EM) section (Fig. 2B) underwent early rupture of lithospheric mantle and extreme thinning of ductile upper crust, which allowed a prolonged presence of upwelling mantle at shallow levels prior to breakup (Lu and Huismans, 2021). Across the BL into the normal magmatic (NM) section (Fig. 2B), the width of extended crust is reduced by at least 100 km, and the size of high-velocity lower-crustal bodies (HVLC) is greatly diminished (Breivik et al., 2017; Gernigon et al., 2020). This implies less corner flow upwelling under a lower extension rate (Lu and Huismans, 2021). Overall, stronger mantle upwelling to the SW would exert differential gravitational stress on the rift, driving northeastward propagation (Fig. 1A).

PEC Structures at the Barents Shelf

As a result of these observations about NAR propagation, there are several questions: (1) Why did the propagation terminate? (2) Did NAR's rotational kinematics create the PEC? (3) How did a rotational continental rift (stage 2) transform into an orthogonal oceanic rift (stage 3)? To answer these questions, we carried out an in-depth study of the SW Barents Shelf, where the propagation of the NAR terminated (Fig. 2B).

Known for its early Eocene sheared margin (Fig. 2D), the SW Barents Shelf is a key area to study the rift-to-drift transition during the opening of the NGS (Fig. 2E). The area is dominated by ancient rift structures from the late Paleozoic to early Mesozoic and underlain by metasediments and gneiss (Faleide et al., 2010). At a few localities (Fig. 2D), mafic-ultramafic bodies are inferred to have been emplaced at shallow depths (Fichler and Pastore, 2022) due to pre-Cenozoic tectonic movements (Gabrielsen, 1984). With the use of an extensive grid of seismic lines and stratigraphy derived from time-depth–converted wellbore data (Fig. 3A), we traced five preglacial horizons across the area (see legend in Fig. 3). The mapping resulted in the identification of two early Eocene features: a horst-and-graben system and a V-shaped anticline, both located northeast of the sheared margin (Fig. 2D).

V-Shaped Anticline

The V-shaped anticline (VA) is composed of the contemporaneously formed Senja Ridge and Finnsnes Ridge (Fig. 2D). The early Eocene age of the two ridges is constrained by the folding of the earliest Eocene and older horizons and by the subsequent onlapping of Ypresian strata on their eastern flanks (Figs. 3B–3D). The southeastern boundary of Finnsnes Ridge is a nearly straight line parallel to the strike of the Troms-Finmark fault complex (TFFC), which implies utilization of a preexisting structure as a tear fault (Fig. 2D). The strongest uplift is recorded at the northern end of Senja Ridge

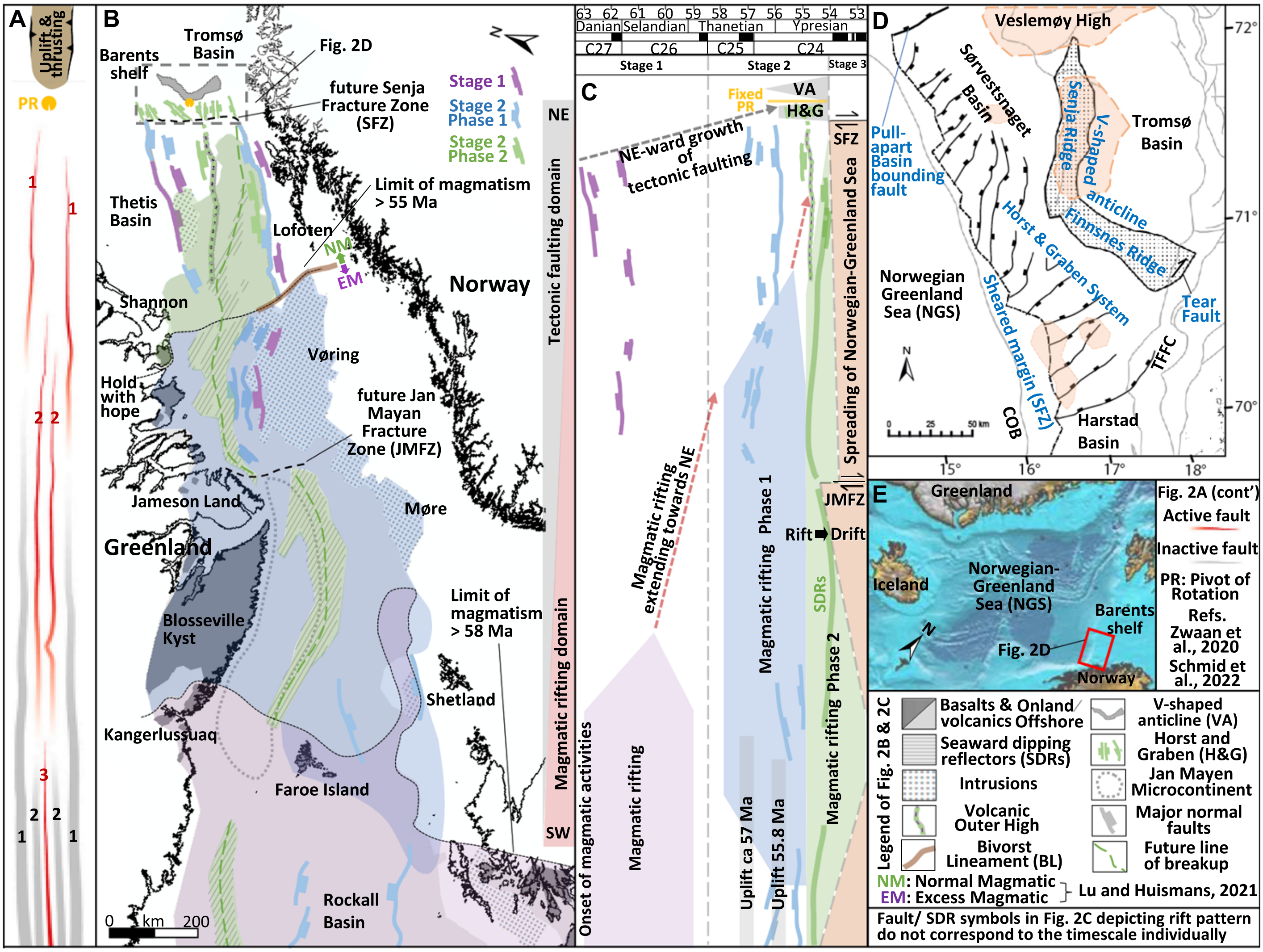

Figure 2. (A) Late-stage propagation and coeval compression of analogue models (numbers—rift generations). PR—pivot of rotation. (B) Early Paleogene tectono-magmatic configurations of Northeast Atlantic Rift (NAR), prior to breakup ca. 54 Ma. (C) Spatiotemporal representation of tectono-magmatic trends of NAR. PR—pivot of rotation; H&G—horst and graben. (D) Early Eocene structures in this study (names in blue): V-shaped anticline; horst and graben system, sheared margin (landward limit indicated by dashed black line), and pull-apart basin's bounding fault (bolded). Other structures of SW Barents Sea are in gray. Mafic/ultramafic bodies are in orange (dashed = elevated; Fichler and Pastore, 2022). COB—continent-ocean boundary, TFFC—Troms-Finnmark fault complex. (E) Location of study area in northeast Atlantic Ocean.

(Fig. 3B) and the southeastern end of Finnsnes Ridge (Fig. 3D), where subaerial erosion created clinoforms prograding eastward. Postuplift downfaulting is recorded on the western flanks of the anticline (Figs. 3B and 3E), which could be related to arrival of the NAR's rift tip (Mondy et al., 2018) and/or subsequent sheared margin formation (Faleide et al., 2010).

Horst-and-Graben System

Our mapping also revealed a horst-and-graben system (H&G) abutting the southwestern tip of the VA (Fig. 2D). Its early Eocene formation was verified by the offsets of the early Eocene horizon (Figs. 3F and 3G). Synrift wedges can be recognized by the cross-fault-plane stratal thickness above the early Eocene horizon. Bounded to the north by a half-graben and to the south by the TTFC, the H&G is crosscut by the NW-SE–trending sheared margin (Fig. 2D), confirming its pre-breakup origin. Downfaulting took place along high-angle normal faults, and block rotation was relatively limited, as indicated by the size of synrift wedges (Figs. 3F and 3G). The horsts west of Senja Ridge seem to share the ridge's NNE-SSW trend (Fig. 2D), implying that the presence of the VA slightly affected the H&G through fault deflection. In general, the H&G shares the same orientation (Fig. 2D) and similar architecture with the late Paleogene rift structures at Thetis Basin and the Lofoten margin (Fyhn et al., 2021; Meza-Cala et al., 2023).

Relationship with the Rotational Kinematics of NAR Propagation

With their earliest Eocene age and their pre-breakup origin confirmed, the H&G and VA can be linked to the NAR propagation (stage 2). Given the coevality, proximity, and similarity in architecture, the H&G can be seen as an integral part of the NAR (Fig. 2B). Since our mapping shows that NAR did not propagate into the Tromsø Basin (Fig. 2D), the southwestern tip of the VA was likely established as a fixed PR (Figs. 2B and 2C), where the NAR's driving force failed to stretch the mafic-ultramafic body (Fig. 2D). In this context, the H&G and the VA represent PEC as postulated by rotational kinematics (Fig. 1B) and analogue models (Fig. 2A). The fact that the two ends of the VA exhibit the greatest uplift, as shown by the subaerial erosion and resultant clinoforms, is a typical manifestation of rotational kinematics, since the linear velocity (V) is the largest at the points farthest away from the PR (Fig. 1A).

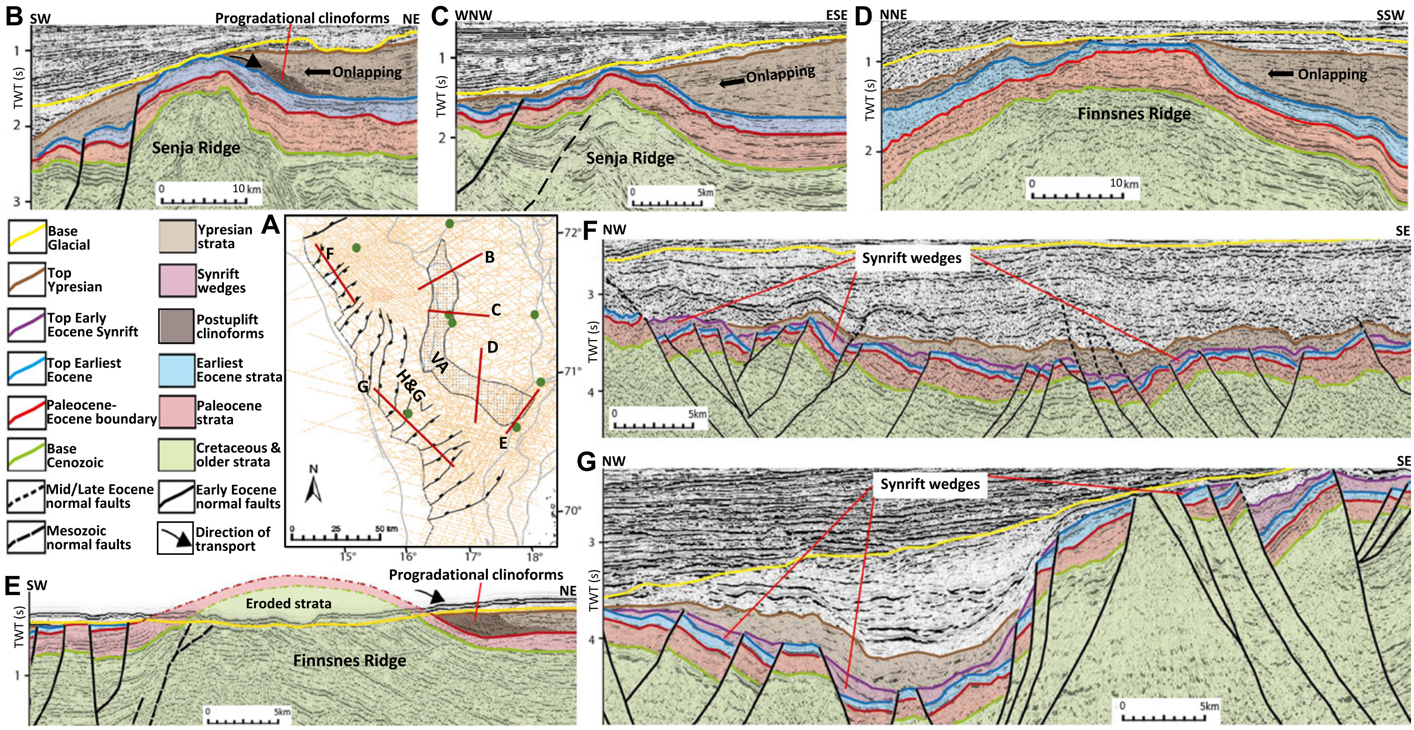

Figure 3. (A) Location of profiles (red), seismic data (yellow), and wellbores (green). VA—V-shaped anticline; H&G—horst-and-graben system. (B–F) Seismic profiles (TWT—two-way traveltime): (B) Senja Ridge (north); (C) Senja Ridge (south), (D) Finnsnes Ridge (east); (E) Finnsnes Ridge (west); (F) horst and graben (north); and (G) horst and graben (south).

DISCUSSION

Role of PEC in the Rift-to-Drift Transition

In the early Eocene, the SW Barents Shelf witnessed a transition from the northeastward-propagating continental rift (NAR; stage 2) into a southwestward-propagating oceanic rift (NGS; stage 3) (Fig. 2C). Here, we suggest that PEC formation played a crucial role in this abrupt change. As the NAR propagated, rifting approached the SW Barents Shelf (Fig. 4A) and eventually encountered the mafic-ultramafic body, which did not yield under the rift's tensile stress. The stalled rift tip then established as a fixed PR, causing forward projection of the rift's driving force and PEC formation (H&G and VA) (Fig. 4B). In this process, the along-axis component was dissipated, and the rift switched to orthogonal extension due to domination of the axis-perpendicular component (Fig. 4C). This rift mode conversion had two effects. First, it forced the rift to assume another energy-effective mode of strain accommodation: strike-slip motion along a preexisting line of weakness. This explains the early Eocene development of the SFZ (Faleide et al., 2010), which is aligned with a Precambrian lineament (Indrevær et al., 2013). Second, it caused a temporary increase in the strain rate at the SFZ. In a rotational setting (stage 2), this locality was subject to less tensile stress and thus had a lower strain rate (*V1*) (Fig. 4B). In an orthogonal setting (stage 3), however, movement of the SFZ promoted uniform upwelling along the axis and hence increased tensile stress and strain rate (*V1′*) at the new rift tip (Fig. 4C). This allowed breakup to occur at the less stretched, normal magmatic margin to the NE while the rest of the NAR was still under crustal thinning (Fig. 4C), leading to apparent propagation of the NGS toward the SW (Franke et al., 2019; Gernigon et al., 2020).

Novel Perspectives on Rift Propagation

Our observations suggest that the along-axis force component and its corresponding mantle flows are strictly necessary for rift propagation. Once this driving force fails to stretch/rupture the crust in front of the rift tip, forward projection of this force around a fixed PR starts to create PEC (Fig. 4D). As PEC formation dissipates the driving force (Fig. 4D), it becomes "self-limiting" once started, and the amount of extension that can be attained is directly correlated to the amount of compression a system is able to accommodate. When the strata or bedrock in front of the rift tip cannot be further deformed, the driving forces will cancel each other out at the "C" sector (arrows pointing at each other, Fig. 1B), leading to termination of propagation. This causality between PEC and termination of propagation, as shown in Figure 4D, can help to explain why PEC is not observed in most propagating rifts. As long as rupture at the rift tip continues, the rift's PR migrates forward (Hey et al., 1980; Brune, 2018), and PEC cannot be formed. Our observation at the SW Barents Shelf thus suggests that more natural examples of PEC may be found at the rift tips of a stalled or terminated propagation.

CONCLUSIONS

The natural example of PEC established through our study is interpreted to have been a key factor in the early Paleogene rift-to-drift transition in the NE Atlantic. Formed at the tip of the NAR, the PEC structures dissipated the along-axis force component required for the propagation. This led to the conversion of rift mode from rotational extension to orthogonal extension, which favored breakup and the development of the sheared margin. Our study suggests that PEC is a natural mechanism that forms during stalling and termination of rift propagation.

ACKNOWLEDGMENTS

We thank Dr. F. Zwaan, Dr. D. Maestrelli, Dr. T. Schmid, and Dr. C. Bulois for the reviews and insightful comments. This study was sponsored by the Department of Geosciences, University of Oslo.

REFERENCES CITED

Abdelmalak, M.M., et al., 2016, Pre-breakup magmatism on the Vøring margin: Insight from new sub-basalt imaging and results from Ocean Drilling Program Hole 642E: Tectonophysics, v. 675, p. 258–274, https://doi.org/10.1016/j.tecto.2016.02.037.

Blischke, A., et al., 2022, Seismic volcanostratigraphy: The key to resolving the Jan Mayen microcontinent and Iceland Plateau rift evolution: Geochemistry, Geophysics, Geosystems, v. 23, https://doi.org/10.1029/2021GC009948.

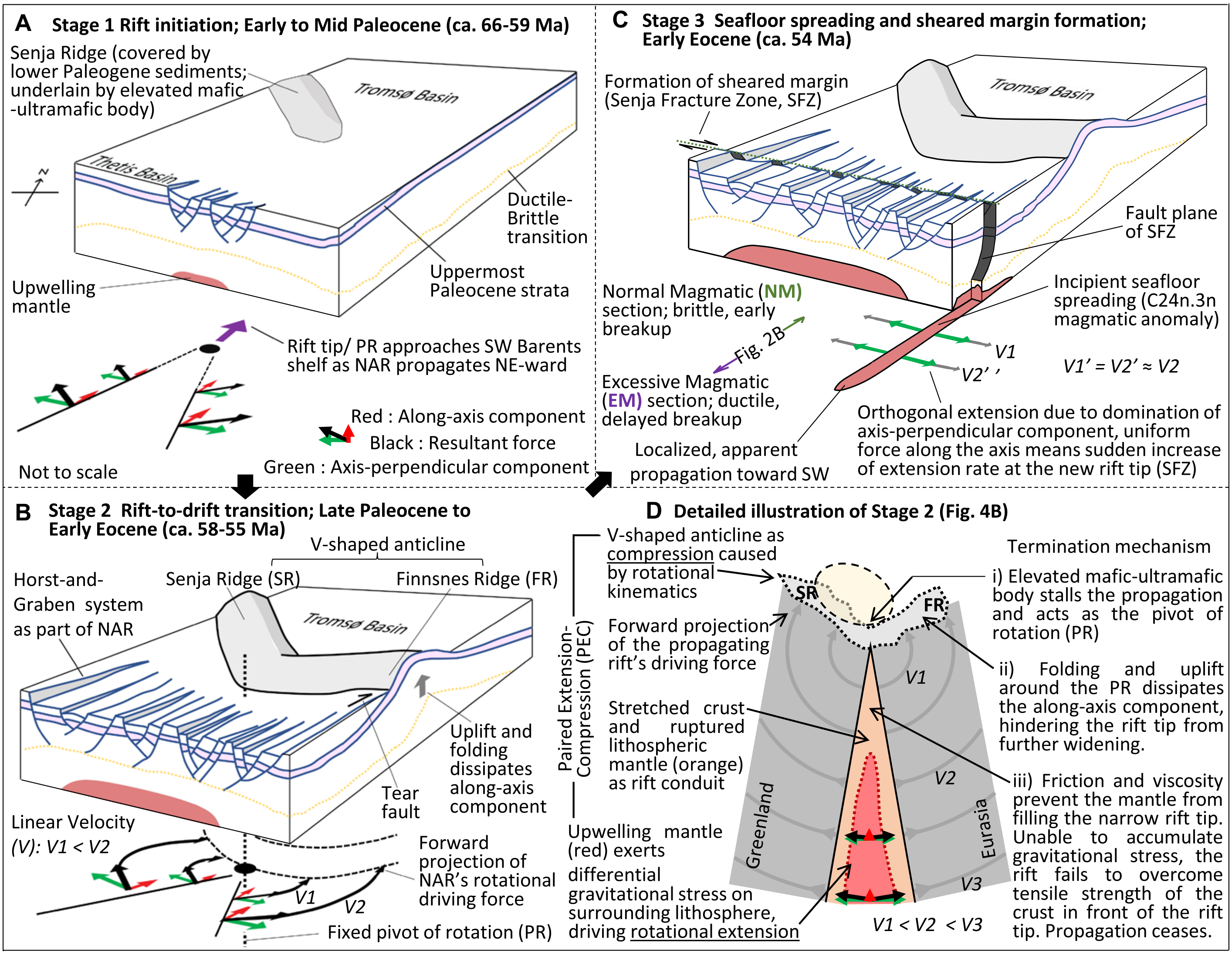

Figure 4. (A–C) Three-stage model of Northeast Atlantic Rift (NAR) evolution: (A) Stage 1: Rift initiation. (B) Stage 2: Rift propagation. (C) Stage 3: Breakup and seafloor spreading. (D) Detailed illustration of stage 2. PR—pivot of rotation; EM—excessive magmatic section; NM—normal magmatic section; PEC—paired extension-compression.

Breivik, A.J., Faleide, J.I., Mjelde, R., Flueh, E.R., and Murai, Y., 2017, A new tectono-magmatic model for the Lofoten/Vesterålen margin at the outer limit of the Iceland plume influence: Tectonophysics, v. 718, p. 25–44, https://doi.org/10.1016/j.tecto.2017.07.002.

Brune, S., 2018, Forces within continental and oceanic rifts: Numerical modeling elucidates the impact of asthenospheric flow on surface stress: Geology, v. 46, p. 191–192, https://doi.org/10.1130/focus022018.1.

Faleide, J.I., Bjlrlykke, K., and Gabrielsen, R.H., 2010, Geology of the Norwegian continental shelf, *in* Bjørlykke, K., ed., Petroleum Geoscience: From Sedimentary Environments to Rock Physics: Berlin, Springer, p. 467–499, https://doi.org/10.1007/978-3-642-02332-3_22.

Fichler, C., and Pastore, Z., 2022, Petrology of the crystalline crust in the southwestern Barents Sea inferred from geophysical data: Norsk Geologisk Tidsskrift, v. 102, 202206, https://doi.org/10.17850/njg102-2-2.

Franke, D., Klitzke, P., Barckhausen, U., Berglar, K., Berndt, C., Damm, V., Dannowski, A., Ehrhardt, A., Engels, M., Funck, T., Geissler, W., Schnabel, M., Thorwart, M., and Trinhammer, P., 2019, Polyphase magmatism during the formation of the northern East Greenland continental margin: Tectonics, v. 38, p. 2961–2982, https://doi.org/10.1029/2019TC005552.

Fyhn, M.B.W., Hopper, J.R., Sandrin, A., Lauridsen, B.W., Heincke, B.H., Nøhr-Hansen, H., Andersen, M.S., Alsen, P., and Nielsen, T., 2021, Three-phased latest Jurassic–Eocene rifting and mild mid-Cenozoic compression offshore NE Greenland: Tectonophysics, v. 815, https://doi.org/10.1016/j.tecto.2021.228990.

Gabrielsen, R.H., 1984, Long-lived fault zones and their influence on the tectonic development of the southwestern Barents Sea: Journal of the Geological Society, v. 141, p. 651–662, https://doi.org/10.1144/gsjgs.141.4.0651.

Gaina, C., Nasuti, A., Kimbell, G.S., and Blischke, A., 2017, Break-up and seafloor spreading domains in the NE Atlantic, *in* Peron-Pinvidic, G., et al., eds., The NE Atlantic Region: A Reappraisal of Crustal Structure, Tectonostratigraphy and Magmatic Evolution: Geological Society, London, Special Publication 447, p. 393–417, https://doi.org/10.1144/SP447.12.

Geissler, W.H., Gaina, C., Hopper, J.R., Funck, T., Blischke, A., Arting, U., Horni, J.A., Peron-Pinvidic, G., and Abdelmalak, M., 2017, Seismic volcanostratigraphy of the NE Greenland continental margin, *in* Peron-Pinvidic, G., et al., eds., The NE Atlantic Region: A Reappraisal of Crustal Structure, Tectonostratigraphy and Magmatic Evolution: Geological Society, London, Special Publication 447, p. 149–170, https://doi.org/10.1144/SP447.11.

Gernigon, L., Franke, D., Geoffroy, L., Schiffer, C., Foulger, G.R., and Stoker, M.S., 2020, Crustal fragmentation, magmatism, and the diachronous opening of the Norwegian-Greenland Sea: Earth-Science Reviews, v. 206, 102839, https://doi.org/10.1016/j.earscirev.2019.04.011.

Hansen, J., Jerram, D.A., McCaffrey, K., and Passey, S.R., 2009, The onset of the North Atlantic Igneous Province in a rifting perspective: Geological Magazine, v. 146, p. 309–325, https://doi.org/10.1017/S0016756809006347.

Hey, R., Duennebier, K., and Morgan, W.J., 1980, Propagating rifts on midocean ridges: Journal of Geophysical Research, v. 85, p. 3647–3658, https://doi.org/10.1029/JB085iB07p03647.

Hindle, D., Fujita, K., and Mackey, K., 2009, Deformation of the northwestern Okhotsk plate: How is it happening?, *in* Stone, D.B., et al., eds., Geology, Geophysics, and Tectonics of Northeastern Russia: A Tribute to Leonid Parfenov: 4. Okhotsk Plate: European Geophysical Union Stephan Mueller Special Publication 4, p. 147–156, https://doi.org/10.5194/smsps-4-147-2009.

Huismans, R., and Beaumont, C., 2011, Depth-dependent extension, two-stage breakup and cratonic underplating at rifted margins: Nature, v. 473, p. 74–78, https://doi.org/10.1038/nature09988.

Indrevær, K., Bergh, S.G., Koehl, J., Hansen, J., Schermer, E.R., and Ingebrigtsen, A., 2013, Post-Caledonian brittle fault zones on the hyperextended SW Barents Sea margin: New insights into onshore and offshore margin architecture: Norsk Geologisk Tidsskrift, v. 93, p. 167–188.

Jolley, D.W., Millett, J.M., Schofield, N., Broadley, L., and Hole, M.J., 2021, Stratigraphy of volcanic rock successions of the North Atlantic rifted margin: The offshore record of the Faroe-Shetland and Rockall basins: Earth and Environmental Science Transactions of the Royal Society of Edinburgh, v. 112, p. 61–88, https://doi.org/10.1017/S1755691021000037.

Larsen, L., Pedersen, A.K., Tegner, C., and Duncan, R.A., 2014, Eocene to Miocene igneous activity in NE Greenland: Northward younging of magmatism along the East Greenland margin: Journal of the Geological Society, v. 171, p. 539–553, https://doi.org/10.1144/jgs2013-118.

Lu, G., and Huismans, R., 2021, Melt volume at Atlantic volcanic rifted margins controlled by depth-dependent extension and mantle temperature: Nature Communications, v. 12, 3894, https://doi.org/10.1038/s41467-021-23981-5.

Lundin, E.R., and Dore, A.G., 2019, Non-Wilsonian break-up predisposed by transforms: Examples from the North Atlantic and Arctic, *in* Wilson, R.W., et al., eds., Fifty Years of the Wilson Cycle Concept in Plate Tectonics: Geological Society, London, Special Publication 470, p. 375–392, https://doi.org/10.1144/SP470.6.

Martin, A.K., 1984, Propagating rifts: Crustal extension during continental rifting: Tectonics, v. 3, p. 611–617, https://doi.org/10.1029/TC003i006p00611.

Meza-Cala, J.C., Tsikalas, F., Abdelmalak, M.M., and Faleide, J.I., 2023, Structural analysis and measured extension in fault complexes along the Lofoten-Vesterålen margin, offshore Norway, in the context of crustal-scale rifting towards breakup in the NE Atlantic: Basin Research, v. 35, p. 1329–1361, https://doi.org/10.1111/bre.12756.

Mondy, L.S., Rey, P., Duclaux, G., and Moresi, L., 2018, The role of asthenospheric flow during rift propagation and breakup: Geology, v. 46, p. 103–106, https://doi.org/10.1130/G39674.1.

Ott, B., and Mann, P., 2015, Late Miocene to recent formation of the Aure-Moresby fold-thrust-belt and foreland basin as a consequence of Woodlark microplate rotation, Papua New Guinea: Geochemistry, Geophysics, Geosystems, v. 16, p. 1988–2004, https://doi.org/10.1002/2014GC005668.

Phipps Morgan, J., and Parmentier, E.M., 1985, Causes and rate-limiting mechanisms of ridge propagation: A fracture mechanics model: Journal of Geophysical Research, v. 90, p. 8603–8612, https://doi.org/10.1029/JB090iB10p08603.

Schmid, T.C., Schreurs, G., and Adam, J., 2022, Characteristics of continental rifting in rotational systems: New findings from spatiotemporal high resolution quantified crustal scale analogue models: Tectonophysics, v. 822, https://doi.org/10.1016/j.tecto.2021.229174.

Stoker, M.S., Holford, S.P., and Hillis, R.R., 2017, A rift-to-drift record of vertical crustal motions in the Faroe-Shetland Basin, NW European margin: Establishing constraints on NE Atlantic evolution: Journal of the Geological Society, v. 175, p. 263–274, https://doi.org/10.1144/jgs2017-076.

Storey, M., Duncan, R.A., and Tegner, C., 2007, Timing and duration of volcanism in the North Atlantic Igneous Province: Implications for geodynamics and links to the Iceland hotspot: Chemical Geology, v. 241, p. 264–281, https://doi.org/10.1016/j.chemgeo.2007.01.016.

Svensen, H., Planke, S., and Corfu, F., 2010, Zircon dating ties NE Atlantic sill emplacement to initial Eocene global warming: Journal of the Geological Society, v. 167, p. 433–436, https://doi.org/10.1144/0016-76492009-125.

Walker, F., Schofield, N., Millett, J., Jolley, D., Hole, M., and Stewart, M., 2022, Paleogene volcanic rocks in the northern Faroe-Shetland Basin and Møre marginal high: Understanding lava field stratigraphy, *in* Chiarella, D., et al., eds., Cross-Border Themes in Petroleum Geology II: Atlantic Margin and Barents Sea: Geological Society, London, Special Publication 495, p. 199–235, https://doi.org/10.1144/SP495-2019-13.

Wallace, L.M., Ellis, S., and Mann, P., 2009, Collisional model for rapid fore-arc block rotations, arc curvature, and episodic back-arc rifting in subduction settings: Geochemistry, Geophysics, Geosystems, v. 10, Q05001, https://doi.org/10.1029/2008GC002220.

Wilkinson, C.M., Ganerød, M., Hendriks, B.W.H., and Eide, E., 2017, Compilation and appraisal of geochronological data from the North Atlantic Igneous Province (NAIP), *in* Peron-Pinvidic, et al., eds., The NE Atlantic Region: A Reappraisal of Crustal Structure, Tectonostratigraphy and Magmatic Evolution: Geological Society, London, Special Publication 447, p. 69–103, https://doi.org/10.1144/SP447.10.

Zastrozhnov, D., Gernigon, L., Gogin, I., Planke, S., Abdelmalak, M.M., Polteau, S., Faleide, J.I., Manton, B., and Myklebust, R., 2020, Regional structure and polyphased Cretaceous–Paleocene rift and basin development of the mid-Norwegian volcanic passive margin: Marine and Petroleum Geology, v. 115, https://doi.org/10.1016/j.marpetgeo.2020.104269.

Zwaan, F., Schreurs, G., and Rosenau, M., 2020, Rift propagation in rotational versus orthogonal extension: Insights from 4D analogue models: Journal of Structural Geology, v. 135, https://doi.org/10.1016/j.jsg.2019.103946.

Printed in the USA